SCIENTIFIC REPORTS

OPEN

SUBJECT AREAS:
CHARACTERIZATION AND ANALYTICAL TECHNIQUES
BATTERIES
IMAGING TECHNIQUES
SOLID-STATE NMR

Received
21 June 2013

Accepted
21 August 2013

Published
5 September 2013

Correspondence and requests for materials should be addressed to R.Q.F. (rfu@magnet.fsu.edu)

Non-Destructive Monitoring of Charge-Discharge Cycles on Lithium Ion Batteries using ^{7}Li Stray-Field Imaging

Joel A. Tang[1,2], Sneha Dugar[1,3], Guiming Zhong[4], Naresh S. Dalal[1,3], Jim P. Zheng[5], Yong Yang[4] & Riqiang Fu[1]

[1]National High Magnetic Field Laboratory, Florida State University, 1800 E. Paul Dirac Drive, Tallahassee, FL, 32310, USA, [2]Department of Chemistry, University of Toronto, Toronto, ON, M5S 3H6, Canada, [3]Department of Chemistry and Biochemistry, Florida State University, [4]State Key Laboratory for Physical Chemistry of Solid Surfaces and Department of Chemistry, College of Chemistry and Chemical Engineering, Xiamen University, PR China, [5]Department of Electrical and Computer Engineering, Florida State University.

Magnetic resonance imaging provides a noninvasive method for *in situ* monitoring of electrochemical processes involved in charge/discharge cycling of batteries. Determining how the electrochemical processes become irreversible, ultimately resulting in degraded battery performance, will aid in developing new battery materials and designing better batteries. Here we introduce the use of an alternative *in situ* diagnostic tool to monitor the electrochemical processes. Utilizing a very large field-gradient in the fringe field of a magnet, stray-field-imaging (STRAFI) technique significantly improves the image resolution. These STRAFI images enable the real time monitoring of the electrodes at a micron level. It is demonstrated by two prototype half-cells, graphite || Li and $LiFePO_4$ || Li, that the high-resolution ^{7}Li STRAFI profiles allow one to visualize *in situ* Li-ions transfer between the electrodes during charge/discharge cyclings as well as the formation and changes of irreversible microstructures of the Li components, and particularly reveal a non-uniform Li-ion distribution in the graphite.

Lithium ion batteries have become an intricate part of our daily routines and are essential in the advancement of alternative energy products. The charge/discharge mechanism of Li-rechargeable batteries is complex and any change to the electrode infrastructure may alter the overall performance. There is still much to know microscopically about the electrochemical processes in the battery, for example, the effects of the electrolyte and the influence of different additives on the interfacial properties of the electrodes. Some changes in structural phases of the electrodes are irreversible leading to battery degradation. A better understanding of these processes and where they occur (e.g. at electrode surface or within) is important to maximize the battery's energy density, power, efficiency and cycle lifetime. Much research has been put forth to determine flaws in a battery's design and underlying structure. Techniques such as X-ray diffraction[1–3], electron microscopy[4,5], scanning probe microscopy[2,6–9] and nuclear magnetic resonance (NMR) spectroscopy[10–12] are being used to examine the molecular and electronic structures, pore and particle size distribution, and surface structures of electrode materials. Although X-ray and microscopy methods can produce detailed surface images, the information attained is often not quantitative. NMR provides a more complete analysis of the bulk material but does not provide spatial information. With most of these techniques, the electrode materials are examined *ex situ*, in which the equilibrium composition of the samples may be altered during extraction/preparation. Thus, obtaining this microscopic structural information under working (*in situ, or operato-*) conditions is very important for understanding electrochemical processes of the electrode materials fully and accurately.

Magnetic resonance imaging (MRI) could provide further insight into battery materials. Its non-invasive nature is attractive because the battery is not destroyed during acquisition. Recently Chandrashekar et al. were able to use MRI to examine the charging process of a Li foil battery cell and quantify the microstructure formation on the surface of the metal electrodes with a resolution of a few hundred microns[13]. Giesecke et al. also demonstrated imaging of a battery phantom by using constant time chemical-shift-selective imaging methods which isolates the electrolyte signal while suppressing other components of the battery material[14]. These imaging approaches are viable for signals that have relatively narrow line-widths, such as Li metal or electrolyte, allowing for long pulses to be applied for high resolution images. However, for materials that exhibit larger line-widths,

such as $LiFePO_4$ or $LiCoO_2$, traditional MRI methods do not appear to be suitable for getting much needed image resolution.

Image resolution is an important parameter for imaging lithium ion batteries since the typical thickness of commercial battery electrodes is ~ 0.100 mm. MRI studies of solid materials are uncommonly performed because exceedingly strong gradients are required to obtain high-resolutions (<0.100 mm). In addition, detection sensitivity also decreases since large bandwidths are required. Stray field imaging (STRAFI) that utilizes very large gradient strengths in the fringe field of a superconducting magnet (typically over 40 times greater than those produced by MRI gradient coils) is an effective imaging method for solid substances, including paramagnetic materials[15–17]. Since STRAFI does not come with chemical shift information, it uses the spin population for imaging, rather than chemical shifts as often used in the conventional MRI experiments. Although the chemical shift provides important information about structural formations, it is difficult to use it as a parameter to achieve high-resolution imaging in complex materials such as batteries when the commonly used high-resolution solid-state NMR techniques (e.g. magic angle spinning) are not applicable.

We have previously reported the feasibility of using high-resolution ^{7}Li STRAFI to examine battery materials[18]. With our home-built STRAFI probe and strong fringe field gradient strength, a resolution of 0.015 mm is achievable and useful for imaging solid materials. Using a battery phantom, we found that the current collectors do not influence the STRAFI profile, implying that the Li^+ movement across battery electrodes during charge/discharge processes can be monitored. In this study, we assembled two prototype $LiFePO_4$ and graphite half-cell cylindrical batteries (Figure 1) and used high-resolution ^{7}Li STRAFI to examine how Li-ions travel *in situ* between electrodes and studied the influence of paramagnetic interactions on STRAFI profiles.

Results

A ^{7}Li STRAFI profile of the graphite||Li half-cell battery in the pristine state is shown in blue in Figure 2. The "peaks" centered at 0.556 and 1.141 mm are associated with the top and bottom planes of the Li foil. Penetration of radio-frequency (RF) into a piece of metal is restricted to a certain depth due to skin effects[19]. Since the foil is oriented parallel to the RF field B_1, the top and bottom planes of the Li foil have large surface areas allowing for more spins to be excited within the STRAFI plane. When the STRAFI plane is within the core of the metal disk, the RF field only excites the outer skin of the foil, not enough to produce a strong signal compared to the top and bottom layers. The signal from 0.508 through 0.556 mm is attributed to the lithium signal from the $LiPF_6$ electrolyte soaked in the separators. The right edge of the peak corresponds to the position of the top edge of the Li foil. The measured thickness of the Li foil is 0.585 mm which is ~ 0.15 mm less than the initial thickness due to the compression in the battery cell assembly. At the left edge of the peak, some small Li signals extending into the graphite were also observed, indicating that some Li ions from the electrolyte diffuse into the graphite layers of the electrode under the pressure in the cell assembly. The small signal at 1.21 mm is believed to be the soft Li foil that was pressed into the screw's flat head slot. The slot is thin enough such that the RF field completely penetrates through the raised foil producing a relatively strong signal. By using a 0.039 mm step-size the edges of the lithium foil in the profile appear to be sharp. Clearly, the STRAFI technique improves the image resolution by an order of magnitude as compared to the traditional MRI techniques[13]. Such a high resolution will aid in determining any slight changes that occur during the charging cycle of the battery.

The graphite||Li half-cell battery was put through a series of discharge/charging cycles between 0.01 V and 3.0 V (Figure S1). The graphite half-cell was first discharged to 0.01 V to ensure that the Li

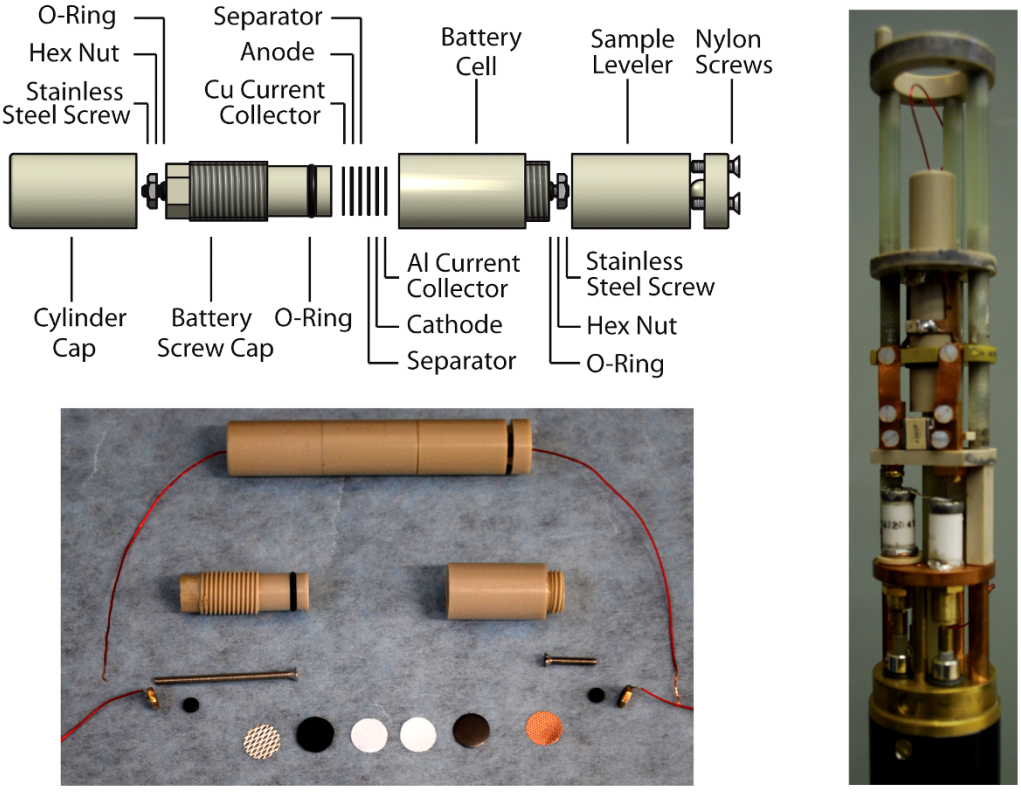

Figure 1 | Schematics of a cylindrical NMR battery cell (left top) used for STRAFI studies. In the bottom of the left panel are the cylindrical battery cell and parts. The home-built *in situ* STRAFI probe is shown in the right panel.

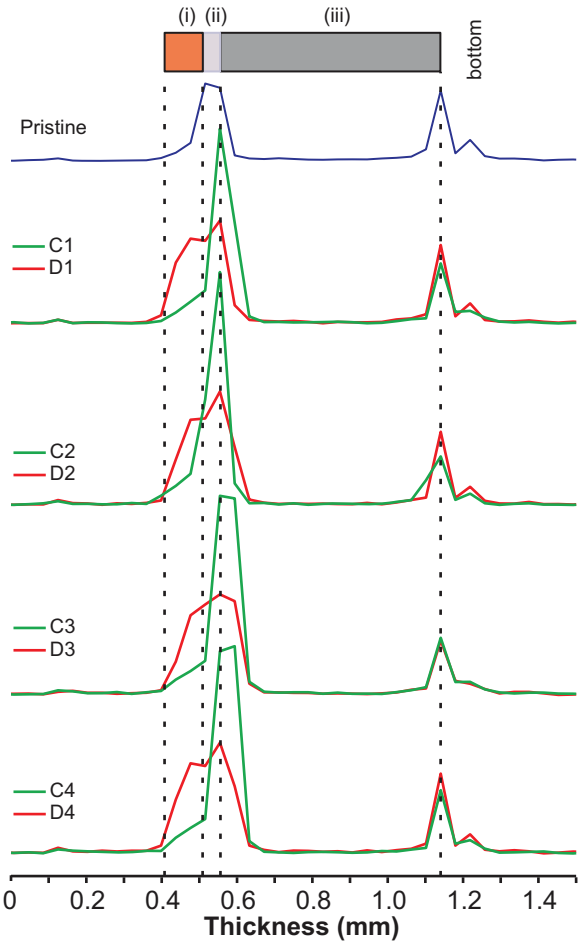

Figure 2 | ^{7}Li STRAFI profiles of a graphite||Li half-cell battery after each charge (C, green) and discharge (D, red) cycle. (i) Graphite electrode, (ii) separator layer consisting of two Celgard 3501 membranes, and (iii) Li foil. Dashed lines and battery assembly above the profile indicates the position of the Li metal foil, separator and graphite electrode as expected in the battery cell.

ions move into the layered graphite structure from the Li foil. After the first discharge (D1) of the battery to 0.01 V, the signal at the graphite electrode significantly increases, as shown in Figure 2. When the battery was charged (C1) to 3.0 V, the Li ions in the layers of the graphite electrode moved back to the Li foil surface, as seen by the reduction of ^{7}Li signal intensity in the graphite region. However, it appears that some residual Li-ions remain in the graphite layers with increasing population towards the interface with the separators. On the other hand, the Li signal at the interface between the separators and the Li foil is more than double compared to the pristine state of the battery. More interestingly, the ^{7}Li signal at the position of 0.595 mm can be observed now, where it was considered inside the Li foil plane and no ^{7}Li signal was observed in both the pristine and discharged states because of the RF skin effect of the metal.

A ^{7}Li STRAFI profile of the $LiFePO_4$||Li half-cell battery in the pristine state is shown in blue in Figure 3. Again, the Li foil is depicted by the two sharp peaks located at 0.585 and 1.095 mm, while the electrolyte in the separators expands from 1.095 to 1.150 mm in the 1D profile. The center of the $LiFePO_4$ electrode, with a thickness of 0.1 mm, was expected to appear at the position of 1.20 mm. However, the center for the $LiFePO_4$ electrode is clearly positioned at 1.385 mm, a shift by 0.18 mm. In addition, the resolution for the $LiFePO_4$ electrode appears to be much worse than that for the Li foil. At the right side of the image, a broad profile with ca. 0.2 mm breadth

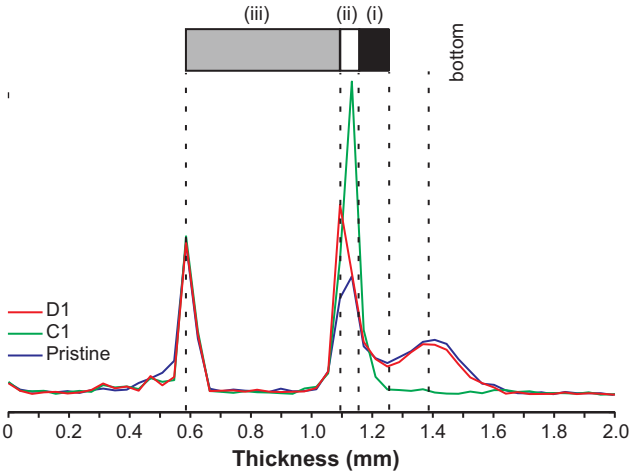

Figure 3 | ^{7}Li STRAFI profiles of a $LiFePO_4$||Li half-cell battery after a charge (C, green) and discharge (D, red) cycle. (i) $LiFePO_4$ electrode, (ii) separator layer consisting of two Celgard 3501 membranes, and (iii) Li foil. Dashed lines and battery assembly above the profile indicates the position of the Li metal foil, separator and $LiFePO_4$ electrode as expected in the battery cell.

at half height corresponds to the $LiFePO_4$ electrode, double the physical thickness of the $LiFePO_4$ electrode being used.

A charge-discharge cycle was applied to examine this $LiFePO_4$||Li half-cell battery using the STRAFI experiment. Since the half-cell begins with a saturation of Li-ions in the cathode material, the battery was initially charged to 4.2 V (Figure S2). During the charge process Li ions *completely* move out of the $FePO_4$ olivine structure, as shown in green in Figure 3, as compared to the graphite electrode where there exist some residual Li-ions when charged. Discharging the battery down to 2.5 V repopulates the $FePO_4$ layers with Li-ions, as shown in red in Figure 3.

Discussion

STRAFI can be used to track the movement of Li ions and the formation and changes of irreversible phases of the Li components during the charge-discharge cycling of a battery. After the graphite||Li half-cell battery is discharged (Figure 2), the newly grown signal compared to the pristine state depicts the movement of Li^{+} ions into the layers of the graphite electrode. The penetration depth of the Li^{+} ions into the graphite electrode is approximately 0.100 mm which is consistent with the thickness of the graphite when it is dry. The peak intensity in the separator region, in particular at the interface with the Li foil, appears to increase. This implies that a thin layer of metal on the surface of the Li foil starts to dissolve into the form of Li-ions during the discharge process so that this layer becomes easier for RF penetration. It is worth noting that the Li distribution in the layers of graphite electrode seems not as uniform as we would expect, although the 0.039 mm image resolution is still not high enough to make this quantitative. After charging the battery the Li ions in the layers of the graphite electrode moved back to the Li foil surface which, in the profile, appears thicker and stronger compared to the pristine state. This implies that the lithium in a thin layer on the surface of the Li foil is dissolved into the electrolyte and move into the graphite during the discharge process, while those Li-ions moving back from the graphite during the charge process do not go back to their metal form. Instead, they form dendritic or mossy Li microstructures on the surface of the Li foil, which allows for a better RF penetration and thus leads to the observation of more Li signals. For the second discharge (D2) and charge (C2) cycle, the Li-ion movements follow a similar trend as the first cycle. While for the third and fourth discharge (D3, D4) and charge (C3, C4) cycles, the signal

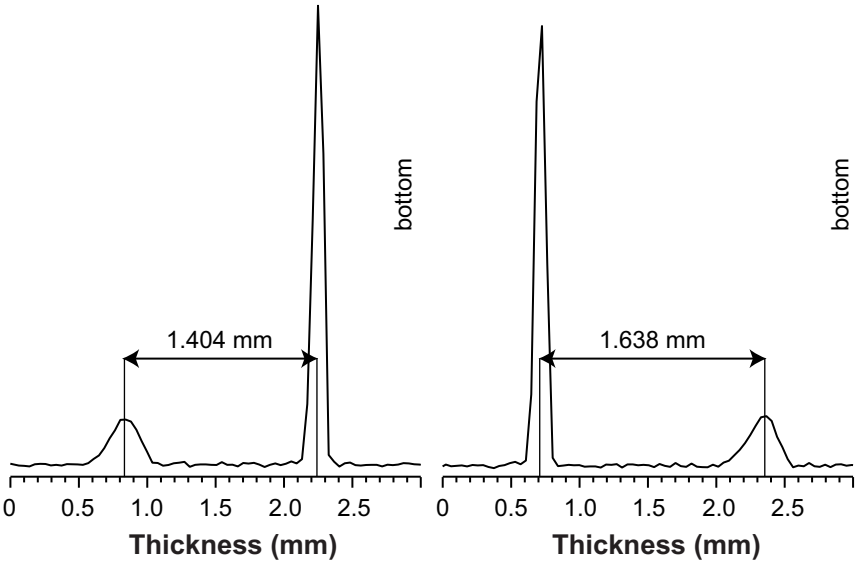

Figure 4 | $LiFePO_4||LiCoO_2$ battery phantom showing the profile displacement due to the presence of paramagnetic Fe nucleus. Left: $LiCoO_2$ was placed at the bottom; Right: $LiFePO_4$ was placed at the bottom.

intensities at the position of 0.595 mm become the same as at the position of 0.556 mm, as if the position for the Li foil surface plane is moved from 0.556 mm to 0.595 mm, indicating that a thin layer of ~ 0.039 mm on the surface of the Li foil is now comprised of the dendritic or mossy Li microstructures. It is worth mentioning again that the Li-ion distribution in the graphite when discharged appears to be non-uniform, with decreasing Li-ion population as the layers moves away from the graphite-separator interface. This may be the effect of the remaining Li-ions in the graphite layers when charged. When these residual Li-ions become immobile, they may limit the passage of the free Li-ions moving into the graphite layers.

The $LiFePO_4||$Li half-cell battery profile (Figure 3) shows typical characteristics of paramagnetic influences on the image. It was previously demonstrated that paramagnetic nuclei may cause the profile to displace from its actual position[17]. Since the $LiFePO_4$ electrode contains paramagnetic Fe nuclei it causes the image to shift due to the interactions with the unpaired electrons. To determine the paramagnetic displacement, a battery phantom consisting of a paramagnetic $LiFePO_4$ and a diamagnetic $LiCoO_2$ electrodes, which are single-side coated on aluminum current collectors and separated by a 1.45 mm Teflon disk, was imaged, as shown in Figure 4. Two STRAFI profiles were measured with two different stacking positions in the magnet for the same electrode phantom. Clearly, the $LiFePO_4$ profile always shifts towards the bottom of the sample, i.e., low field direction, no matter if $LiFePO_4$ is placed on the top or at the bottom by flipping the same phantom. The breadth of the $LiFePO_4$ profile at half-height is just over 0.23 mm which is about double the actual physical thickness of 0.1 mm. The increase in thickness is associated with the paramagnetic interactions which span a wide chemical shift range allowing the signals to spread over a large frequency range. For instance, one micron resolution corresponds to 1.12 kHz in frequency under our experimental condition (i.e. the magnetic field of 11.2 T and the field gradient of 72 T/m). If a signal has a linewidth of 0.14 MHz, it will span over 0.117 mm spatially. It is worth noting that, with such a broad-line, it is extremely difficult, if not impossible, to use the traditional MRI techniques for getting high-resolution images. In comparison, the measured thickness for the $LiCoO_2$ electrode is approximately 0.09 mm, which is consistent with the actual physical breadth of the $LiCoO_2$ electrode used.

By measuring the distance Δ_m between the centers of the $LiFePO_4$ and $LiCoO_2$ profiles, we can accurately determine the paramagnetic shift of the $LiFePO_4$ electrode material:

$$\Delta_m = \Delta_a \pm \Delta_s \quad (1)$$

where Δ_a refers to the actual (physical) distance between the electrodes and Δ_s corresponds to the displacement by the paramagnetic $LiFePO_4$. When the $LiFePO_4$ electrode is at the bottom and top side, this equation takes the plus and minus sign, respectively. In Figure 4, the measured distance between the electrodes is 1.638 and 1.404 mm, when the $LiFePO_4$ electrode is placed at the bottom and top, respectively. Thus, the displacement Δ_s was calculated to be 0.117 mm, corresponding to a shift of −0.14 MHz at the gradient strength of 72 T/m. Therefore, it is straightforward to determine the displacement in paramagnetic solids using STRAFI profiles.

The movement of Li ions in and out of the $FePO_4$ olivine structures of the $LiFePO_4||$Li half-cell battery was also monitored. After the charge process, the residual Li-ions of the dissolved Li foil form the dendritic or mossy Li microstructures on the surface of the Li metal foil, as can also been seen from the STRAFI profile that the amount of Li-ions increase at the surface of the Li foil and in the separators. When discharging the battery we notice from the STRAFI profile in Figure 3 that the Li population in the $FePO_4$ layers is less than its pristine state, while more Li ions remain on the surface of the Li foil and in the separators. This implies that the dendritic or mossy Li microstructures on the surface of the Li foil are not reversible and would be accumulated as the charge/discharge processes go on.

It is worth noting that in our studies we use the Li foil as an anode in the half-cell batteries. Apparently, the Li ions that moved back from the electrodes during the charge processes cannot intercalate into the bulk of the Li foil, thus forming the irreversible dendritic or mossy Li microstructures on the surface of the Li foil, as also observed in a symmetric lithium cell by Jerschow and his coworkers[13]. The dendritic microstructures in the half-cell batteries studied here have a thickness of 0.039 mm on the surface of the Li foil.

In conclusion, we have used a high-resolution STRAFI technique to monitor the Li-ions movement *in situ* across the electrodes in lithium ion batteries during charge-discharge processes. Specifically, two prototype half-cell batteries, i.e., graphite||Li and $LiFePO_4||$Li, were investigated. In the graphite||Li half-cell battery, a thin layer (~0.039 mm) on the surface of the Li foil provides the source of the Li ions to intercalate into the graphite during the discharge process. However, those Li ions do not go back to their initial state. Instead, they form dendritic or mossy Li microstructures on the surface of the Li foil during the charge process. Interestingly, there

are some residual Li ions remaining in the graphite layers with population building up close to the interface with the separators. It was found that there exist a small amount of Li ions remaining in the electrode materials such as $Li_xV_2O_5$ through *ex situ* studies[20,21]. However, high-resolution STRAFI images permit us to locate the position of the residual Li ions remaining in the electrode for the first time. These residual Li ions in the graphite could be the cause of the non-uniform distribution of the Li ions in the graphite layers. While for the $LiFePO_4$||Li half-cell battery where the source of the Li ions is from the $LiFePO_4$ cathode, there are no remaining Li ions in the $FePO_4$ olivine structure when charged. All of the Li ions from the $FePO_4$ cathode move to the anode and form the irreversible dendritic or mossy Li microstructures on the surface of the Li foil during the charge process. Although the image resolution for the $LiFePO_4$ material is relatively poor in the presence of paramagnetic Fe nuclei, the displacement due to its paramagnetic shift could be beneficial. With proper positioning, this paramagnetic shift can displace the profile away from the separators, effectively increasing the gap between the anode and cathode to compensate for the loss of image resolution in the cathode material. The ability to image paramagnetic cathode materials is particularly important, since many cathode materials either contain paramagnetic components (e.g. $LiFePO_4$) or exhibit inter-conversion between charge states upon Li intercalation (e.g. $Li_xV_2O_5$)[22], some of which become paramagnetic. Overall, the ability to detect where, when and which conditions the irreversible lithium components are accumulating in the electrodes/electrolyte during the charge/discharge electrochemical processes will be very useful for material scientists, providing them with a guideline to improve the materials/devices. It is anticipated that this alternative non-invasive diagnostic tool will have a direct and significant impact in the area of energy storage materials (such as Li-ion batteries and Li-ion supercapacitors) as well as catalytic materials (e.g. distribution and agglomerate process of electrocatalysts in fuel cells).

Methods

Electrode preparation. Single sided $LiFePO_4$ and graphite electrodes were purchased from MTI Corporation (www.mtixtl.com). $LiFePO_4$ electrode films are on aluminum current collectors and have a material thickness of 0.1 mm. Graphite electrodes are coated on copper current collectors and have a thickness of 0.1 mm. The Li foil with 0.75 mm thickness was purchased from Sigma-Aldrich and used as obtained. The electrodes were cut into 6.35 mm disks in diameter and dried in a vacuum oven at 120°C overnight prior to cell assembly.

STRAFI battery cell. The cylindrically designed battery cell used for *in situ* battery studies, as shown in Figure 1 is based on a design by Poli et al[23]. The main battery cell, made of polyetheretherketone (PEEK) plastic, has an opening with a diameter of 6.75 mm. The battery is sealed with a PEEK screw cap equipped with a Buna O-ring to seal the system. Through holes down the center of the cap and cell allow for screws to make contact between the current collector and electrical leads. The top and bottom of the cell are sealed with Buna O-rings and compressed with brass hex nuts to which flexible copper wire is attached.

Cell assembly. The battery cells were thoroughly cleaned and dried prior to assembly. Half-cell batteries (graphite||Li and $LiFePO_4$||Li) were assembled in an Ar filled glove box with O_2 and H_2O content less than 1 ppm. Each cell was assembled by first inserting an electrode and two Celgard® 3501 Specialty Microporous Membrane (www.celgard.com) separators, followed by adding 4–5 drops of 1 M $LiPF_6$ in 1 : 1 (v/v) ethylene carbonate and ethyl methyl carbonate electrolyte. Finally the second electrode was inserted. The battery cells were caped, tightly pressed and left overnight for electrolyte impregnation.

Battery charge/discharge procedure. Charge/discharge cycles for *in situ* studies were performed using a Gamry Reference 600 Potentiostat/Galvanostat. The batteries were charged using a constant current (~30 μA) up to a desired voltage maximum at which charging continued at constant voltage until the current dropped back down to 10% of its original value. A constant current (~30 μA) was used to discharge the batteries to their desired voltage. The images were acquired once the cells had reached their charge/discharge voltages (0.01/3.0 V for graphite||Li and 2.5/4.2 V for $LiFePO_4$||Li).

STRAFI. All STRAFI experiments were conducted on a Magnex 19.6 T ultra-narrow bore (31 mm) superconducting magnet using a Bruker DRX console. An intricate part of STRAFI experiments is determining the most uniform and strongest gradient region in the stray magnetic field of the superconducting magnet[24,25]. The sweet spot for the STRAFI position was found at 11.2 T with a gradient strength of 72 T/m. $[90_x\text{-}\tau_1\text{-}(90_y\text{-}\tau_2\text{-acq-}\tau_2\text{-})_N]$ quadrupole echo sequence was used with N = 8. Pulse calibrations were performed using a concentrated sample of LiBr in D_2O and further refined using the battery material in the presence of metal foils. 90° flip angles were confirmed using methods described by Randall et. al[26]. Rectangular pulses with a 90° pulse length of 29 μs were used in the echo sequence. Inter pulse delays for τ_1 and τ_2 were 9 and 12.5 μs, respectively. The translational movement of the sample was controlled using a stepper motor. The distance of travel by a single motor step was calibrated by measuring the number of steps required to move a total distance of 1 cm. One motor step is equivalent to translating the sample by 1.56 μm. The sample was initially brought to a predetermined reference point and then raised to a starting position to be imaged. With each imaging step the sample was moved up by 0.039 mm. After the movement settled down for 300 ms, the quadrupole echo sequence was applied to acquire a number of echoes. Immediately after, the stepper motor translated the sample to the next position for signal acquisition and repeated this movement until the last point to be imaged was reached. A recycle delay of 0.3 s was implemented prior to the stepper motor moving the sample back to the start position and repeated this procedure for signal accumulation. A short recycle delay was employed because only a thin slice of spins is excited and the required time to excite the same position after the sample has been swept thorough is often longer than the longitudinal relaxation of the sample. A home built triggering device was used to control such movements in synchronization with the pulse sequence used for the STARFI experiments. For each profile, the sample was scanned 1600 times requiring a total of 113 minutes to accumulate the signal. A MATLAB (v7.8.0) script was used to convert the echo intensities into the STRAFI profiles. A more complete description of experimental procedures can be found in Ref. 18.

1. Balasubramanian, M., Sun, X., Yang, X. Q. & McBreen, J. In situ x-ray diffraction and x-ray absorption studies of high-rate lithium-ion batteries. *J Power Sources* **92**, 1–8 (2001).
2. Shearing, P. R. *et al.* Characterization of the 3-dimensional microstructure of a graphite negative electrode from a Li-ion battery. *Electrochem Commun* **12**, 374–377 (2010).
3. Yoon, W. S. *et al.* In situ x-ray absorption spectroscopic study on $LiNi_{0.5}Mn_{0.5}O_2$ cathode material during electrochemical cycling. *Chem Mat* **15**, 3161–3169 (2003).
4. Andersson, A. M. *et al.* Surface characterization of electrodes from high power lithium-ion batteries. *J Electrochem Soc* **149**, A1358–A1369 (2002).
5. Delmas, C. *et al.* Lithium deintercalation in $LiFePO_4$ nanoparticles via a domino-cascade model. *Nat Mater* **7**, 665–671 (2008).
6. Kalinin, S. *et al.* Li-ion dynamics and reactivity on the nanoscale. *Mater Today* **14**, 548–558 (2011).
7. Kalinin, S. V. & Balke, N. Local electrochemical functionality in energy storage materials and devices by scanning probe microscopies: Status and perspectives. *Adv Mater* **22**, E193–E209 (2010).
8. Lim, C., Yan, B., Yin, L. & Zhu, L. Simulation of diffusion-induced stress using reconstructed electrodes particle structures generated by micro/nano-CT. *Electrochim Acta* **75**, 279–287 (2012).
9. Wilson, J. R., Cronin, J. S., Barnett, S. A. & Harris, S. J. Measurement of three-dimensional microstructure in a $LiCoO_2$ positive electrode. *J Power Sources* **196**, 3443–3447 (2011).
10. Carewska, M. *et al.* Electrical conductivity and Li-6, Li-7 NMR studies of $Li_{1+y}CoO_2$. *Solid State Ionics* **93**, 227–237 (1997).
11. Key, B. *et al.* Real-time NMR investigations of structural changes in silicon electrodes for lithium-ion batteries. *J Am Chem Soc* **131**, 9239–9249 (2009).
12. Grey, C. P. & Dupre, N. NMR studies of cathode materials for lithium-ion rechargeable batteries. *Chem Rev* **104**, 4493–4512 (2004).
13. Chandrashekar, S. *et al.* Li-7 MRI of Li batteries reveals location of microstructural lithium. *Nat Mater* **11**, 311–315 (2012).
14. Giesecke, M., Dvinskikh, S. V. & Furo, I. Constant-time chemical-shift selective imaging. *J Magn Reson* **226**, 19–21 (2013).
15. Randall, E. W. H-1 and F-19 magnetic resonance imaging of solid paramagnetic compounds using large magnetic field gradients and hahn echoes. *Solid State Nucl Magn Reson* **8**, 173–178 (1997).
16. Randall, E. W., Samoilenko, A. A. & Fu, R. Q. STRAFI imaging of paramagnetic solids: P-31 paramagnetic displacements. *Magn Reson Chem* **40**, 93–95 (2002).
17. Randall, E. W., Samoilenko, A. A. & Nunes, T. NMR imaging of paramagnetic solids in the high-field gradient approximation with the STRAFI method. *J Magn Reson Ser A* **116**, 122–124 (1995).
18. Tang, J. A. *et al.* Solid-state STRAFI NMR probe for material imaging of quadrupolar nuclei. *J Magn Reson* **225**, 93–101 (2012).
19. Bhattacharyya, R. *et al.* In situ NMR observation of the formation of metallic lithium microstructures in lithium batteries. *Nat Mater* **9**, 504–510 (2010).
20. Stallworth, P. E. *et al.* Magnetic resonance studies of chemically intercalated $Li_xV_2O_5$ (x = 1.16 and 1.48). *Solid State Ionics* **146**, 43–54 (2002).
21. Fu, R. *et al.* High-resolution ^{7}Li solid-state NMR study of $Li_xV_2O_5$ cathode electrodes for Li-rechargeable batteries. *J Phys Chem B* **107**, 9730–9735 (2003).
22. Ma, Z. *et al.* Investigation of Li-$Li_xV_2O_5$ rechargeable batteries at different charged states using NMR spectroscopy. *J New Mat Electr Sys* **7**, 269–273 (2004).

23. Poli, F., Kshetrimayum, J. S., Monconduit, L. & Letellier, M. New cell design for *in situ* NMR studies of lithium-ion batteries. *Electrochem Commun* **13**, 1293–1295 (2011).
24. Hugon, C., Aubert, G. & Sakellariou, D. An expansion of the field modulus suitable for the description of strong field gradients in axisymmetric magnetic fields: Application to single-sided magnet design, field mapping and STRAFI. *J Magn Reson* **214**, 124–134 (2012).
25. Van Landeghem, M., Bresson, B., Blumich, B. & de Lacaillerie, J. B. D. Micrometer scale resolution of materials by stray-field magnetic resonance imaging. *J Magn Reson* **211**, 60–66 (2011).
26. Randall, E. W. A convenient method for calibration of the pulse-length in high field-gradients using hahn echo-trains. *Solid State Nucl Magn Reson* **8**, 179–183 (1997).

Acknowledgements

We are grateful for financial support from the User Collaboration Grant Program (UCGP) at the National High Magnetic Field Laboratory (NHMFL) which is supported by the NSF Cooperative Agreement DMR-1157490, the State of Florida, and the U.S. Department of Energy. Y.Y. would also like to thank financial support from National Natural Science Foundation of China (Grants 21233004) and China National Basic Research Program (973 Program, No 2011CB935903). We thank Wanjun Cao at the College of Engineering at Florida State University for discussions and support in making battery materials and cell assembly.

Author contributions

J.A.T. and S.D. conducted STRAFI experiments, prepared battery cells, and carried out data processing; G.Z., Y.Y. and J.P.Z. provided useful insight and discussion into battery cell assembly; Y.Y., J.P.Z. and N.S.D. revised manuscript. R.F. attained financial support and initialized STRAFI experiments; J.A.T., S.D. and R.F. wrote and revised the manuscript.

Additional information

Supplementary information accompanies this paper at http://www.nature.com/scientificreports

Competing financial interests: The authors declare no competing financial interests.

How to cite this article: Tang, J.A. *et al*. Non-Destructive Monitoring of Charge-Discharge Cycles on Lithium Ion Batteries using ^{7}Li Stray-Field Imaging. *Sci. Rep.* **3**, 2596; DOI:10.1038/srep02596 (2013).